A 2-D Diesel Particulate Regeneration Model

Abstract: Diesel particulate filter (DPF) has been widely applied as the efficient way to reduce the soot emissions from diesel engines. The oxidation of the accumulated soot layer in the particulate filter, known as DPF regeneration, plays a crucial role in the diesel engine operation. It is important to understand the characteristics and fundamentals of this process. A 2D time-dependent diesel particulate filter (DPF) regeneration model has been formulated through FEMLAB multiphysics. Momentum balances, mass balance, energy balance and catalytic chemical reactions have been considered in this model. The distributions of exhaust species concentration, bulk gas temperature, soot layer thickness along the filter channel have been investigated. The sensitivity of the soot layer thickness distribution relative to the exhaust temperature has also been analyzed.

I. Introduction

The diesel particulate filter (DPF) is a designed device to collect diesel particulate emissions. The wall-flow monolith DPF is currently the most effective device to reduce diesel particulate emissions (mainly the soot emissions) providing the highest filtration efficiency (more than 90% [1]) with the least pressure drop. Figure 1 [2] shows a typical structure for the wall-flow monolith DPF. While exhaust gases pass through the porous walls between the channels, some of the particulates can be filtered on the wall due to the pore sizes of the walls. The accumulated soot particulates will form soot layers on the walls. As too much particulates are accumulated on the wall, the backpressure in the exhaust system will rise which will increase the engine fuel consumption and reduce the engine power. Thus, it is necessary to clean the filter by oxidizing the collected soot particulates in the DPF. This process is known as regeneration. Numerous regeneration techniques [3,4, 5,6] have been proposed during the last 20 years. Catalytic regeneration (fuel doping [7,8] or a catalytically filter [9,10]) has been shown as the most effective technique. The purpose of this project is to formulate a simulation model in FEMLAB to get a better understanding of the regeneration process and the factors affecting the regeneration behavior.

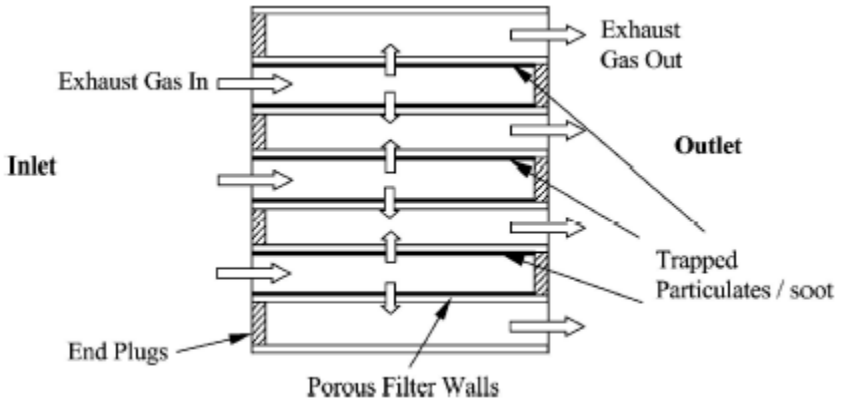

Fi g. 1 S chematic of a monolithic wall-flow DPF from Law M.C. *et al.*

Bissett and Shadman [11,12] reported the first 1-D models for DPF regeneration. Based on their models, Garner and Dent [13] developed a generalized time-dependent DPF model which was not only applicable to wall-flow DPF but also applicable to fibrous DPF. In their model both soot oxidization and gas phase reaction were considered. Mass balance and energy balance for both soot and exhaust gas stream were developed. Bissett's work

has also been extended by Koltsakis,G.*e tal.,* [14],supported by experiment validation of high space velocity thermal regeneration events. Opris and Johnson [15] developed a 2-D DPF regeneration model and found that regeneration process can proceed from upstream to the downstream in the filter channels and regeneration wave returned back to upstream after soot was completely oxidized at the downstream end. Knoth *et al.* built a 2-D transport and reaction model in catalytic wall-flow filters by using FEMLAB. However, only a generic first order global reaction was considered in their model. They also didn't consider the gas phase reaction. Konstandopolous *et al.* [16] developed a 3-D CFD model, through which the temperature distribution can be studied for the whole DPF. Although 2-D and 3-D models can give a clearer description of the DPF regeneration process, aforementioned models have not taken detailed sub models of multiple chemical reactions that occur during the regeneration process into account. Based on this point of view, Law *et al.* [2] developed a 1-D DPF regeneration model with a multi-step chemical reaction scheme. In their model, detailed chemical reaction kinetics was studied. They investigated various exhaust gas species concentration effects on the regeneration process. Based on this model, Law *et al.* [17] also investigated the soot properties, such as soot activation energy, bulk density and porosity, effects on the regeneration behavior. Konstantas *et al.* [18] formulated a validated 1-D model [19,20,21] in MATLAB/Simulink environment investigating the engine operating conditions effects on wall temperature and pressure drop across the filter.

The current work will focus more on formulating a 2-D time-dependent catalytic wall-flow monolith DPF regeneration model in FEMLAB described by mass, energy and momentum balances coupled with detailed chemical reaction kinetics based on the reviewed models.

II. Governing Equations& Model Formulation

The two-dimensional model of the wall-flow monolith filter consists of one inlet channel (domain $\Omega_{1,}$ $\Omega_{5)}$, the soot layer (domain $\Omega_{2)}$, the porous wall (domain $\Omega_{3)}$, and the outlet channel (domain Ω_4 , $\Omega_{6)}$. Figure 2. shows the computational domains and boundaries for this 2D model.

The flow in domains $\Omega_{1,}$ $\Omega_{4,}$ $\Omega_{5,}$ Ω_6 is modeled by the Navier-Stokes equation combined with the continuity equation.

$$\rho \frac{\partial \mathbf{u}}{\partial t} + \rho(\mathbf{u} \cdot \nabla)\mathbf{u} = -\nabla p + \eta \nabla^2 \mathbf{u} \qquad (1)$$

$$\frac{\partial \rho}{\partial t} + \nabla \cdot (\rho \mathbf{u}) = 0 \qquad (2)$$

In the soot layer ($\Omega_{2)}$ and porous wall (Ω_3), the flow field is described by a combination of Brinkman equation and continuity equation.

$$\rho \frac{\partial \mathbf{u}_1}{\partial t} - \eta \nabla^2 \mathbf{u}_1 + \frac{\eta}{k} \mathbf{u}_1 = -\nabla p_1 \qquad (3)$$

$$\frac{\partial \rho}{\partial t} + \nabla \cdot (\rho \mathbf{u}_1) = 0 \qquad (4)$$

, where η is dynamic viscosity and k is the permeability of the porous structure.

Heat transfer is described by an energy balance which is valid in all four domains.

$$\rho C_p \frac{\partial T}{\partial t} + \nabla \cdot (-\lambda \nabla T + \rho C_p T \mathbf{u}) = Q \qquad (5)$$

, where λ is thermal conductivity and Q is the source term.
Mass balance for a specific species is described by Maxwell-Stefan mass diffusion and convection, which is also valid for all of the four domains.

$$\frac{\partial \rho \omega_i}{\partial t} + \nabla \cdot (\mathbf{j}_i + \rho \omega_i \mathbf{u}) = R_i \qquad (6)$$

$$\mathbf{j}_i = -\rho_i \sum_{k=1}^{n} \widetilde{D}_{ik} \mathbf{d}_k \qquad (7)$$

, where R_i represents the reaction rate for i species, ω_i represents mass fraction of species i. Detailed boundary conditions for the above governing equations have been described in Table 1~3. The soot layer needs to be removed through carbon oxidation reactions to keep the filter in working condition. A detailed description of the chemical reactions has been included in this model. The following reactions will be considered in this model.

$C + O_2 \rightarrow CO_2$ (R1) $\quad C + 0.5O_2 \leftrightarrow CO$ (R2)

$C + +4C_e \rightarrow 2C_{e2}O_3 + CO_2$ (R3) $\quad C + 2C_eO_2 \rightarrow C_{e2}O_3 + CO$ (R4)

$C_{e2}O_3 + 0.5O_2 \rightarrow 2C_eO_2$ (R5)

Reaction rates can be described as $r_i = K_{fi} \prod_{j=1}^{N} C_j^{\nu'_{ji}} - K_{ri} \prod_{j=1}^{N} C_j^{\nu''_{ji}}$ (8)

The heat source due to chemical reactions is: $Q = \sum_{i=1} r_i \Delta H_i$ (9)

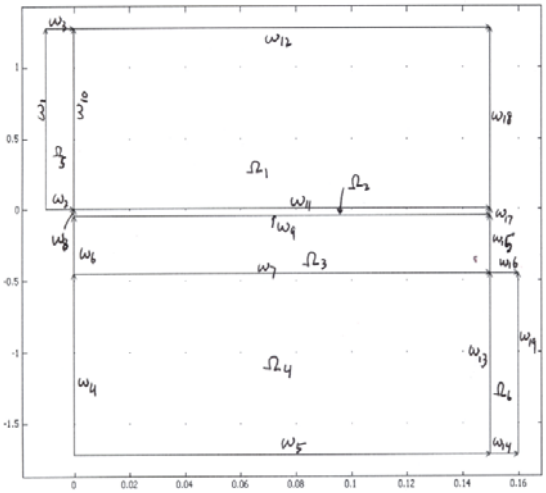

Fig. 2 Geometry structure of the filter

Table 1 Boundary conditions for the flow field

Navier-Stokes equations	
ω_1	$\mathbf{u}=\mathbf{u}_0$
ω_7, ω_{11}	$P_{Navier\text{-}Stokes}=P_{Brinkman}$
$\omega_2, \omega_{18}, \omega_4, \omega_{16}$	$\mathbf{u}=0$
$\omega_3, \omega_{12}, \omega_{16}, \omega_5, \omega_{14}$	$\mathbf{n}\cdot\mathbf{u}=0 \quad \mathbf{t}\cdot\eta(\nabla\mathbf{u})=0$
ω_{19}	$P_0=0$; $\mathbf{t}\cdot\mathbf{u}=0$; $\mathbf{n}\cdot\eta(\nabla\mathbf{u})=0$
Brinkman equations	
ω_7, ω_{11}	$\mathbf{u}_{Navier\text{-}Stokes}=\mathbf{u}_{Brinkman}$
$\omega_6, \omega_8, \omega_{15}, \omega_{17}$	$\mathbf{u}=0$

III. Solution

Several important results solved from the current model have been listed in figure 3, 4, 5, 6, 7, 8 and 9. Figure 3 and figure 4 are the bulk gas temperature distribution in the filter at t=200s and t=500s respectively. These two pictures showed a trend that reaction first started at the downward at the end of the filter and then propagates back to the upstream. This trend has also been confirmed from the comparison of the soot layer and filter wall pressure distribution in figure 5 and figure 6. As can be seen in these two pictures, as time goes on, the soot at the end of the filter is burned off sooner. Therefore, at t=500s, there has been very little pressure drop across the soot layer that can be observed at the end of the filter, which indicates the soot layer has almost been burned off at this side. Figure 9 shows the soot layer thickness distribution along the filter at several different times, which also shows the aforementioned trend. Figure 7 and figure 8 have shown the distribution of oxygen and carbon dioxide in the filter. Again, more oxygen and carbon dioxide are found downstream at the end of the filter indicating faster reaction rate on this side of the filter.

Table 2 Boundary conditions for energy balance

ω_1	$T=T_0=400k$
ω_2, ω_3, ω_4, ω_5 ω_6, ω_{12}, ω_{13}, ω_{14}, ω_{16}, ω_{17}	$\mathbf{n}\cdot\mathbf{q}=0$; $\mathbf{q}=-\lambda\nabla T+\rho C_P T\,\mathbf{u}$
ω_{19}	$\mathbf{n}\cdot\mathbf{q}=0$; $\mathbf{q}=-\lambda\nabla T$

Table 3 Boundary conditions for mass balance

ω_1	$w_i=w_{i0}$
ω_2, ω_3, ω_4, ω_5 ω_6, ω_{12}, ω_{13}, ω_{14}, ω_{16}, ω_{17}	$\mathbf{n}\cdot\mathbf{N}_i=0$; $\mathbf{N}_i=-\rho w_i\sum D_{ik}(\nabla x_k-w_k)\nabla p/p)+\rho w_i\,\mathbf{u}$
ω_{19}	$\mathbf{n}\cdot\mathbf{N}_i=0$; $\mathbf{N}_i=-\rho w_i\sum D_{ik}(\nabla x_k-w_k)\nabla p/p)$

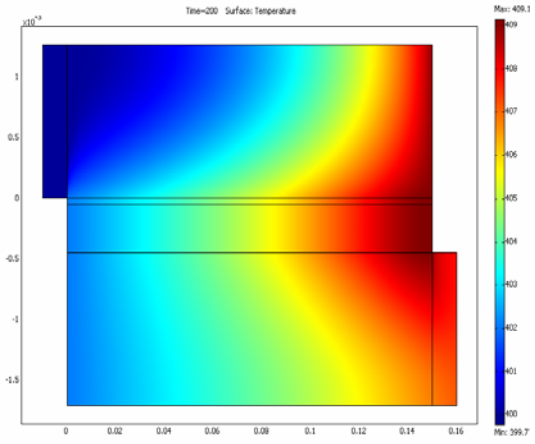

Fig.3 Global Temperature distribution at t=200s

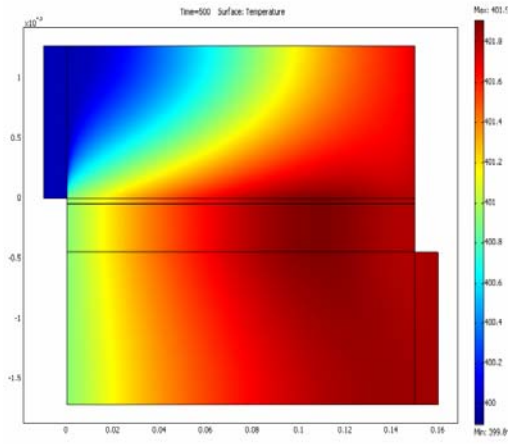

Fig. 4 Global Temperature distribution at t=500s

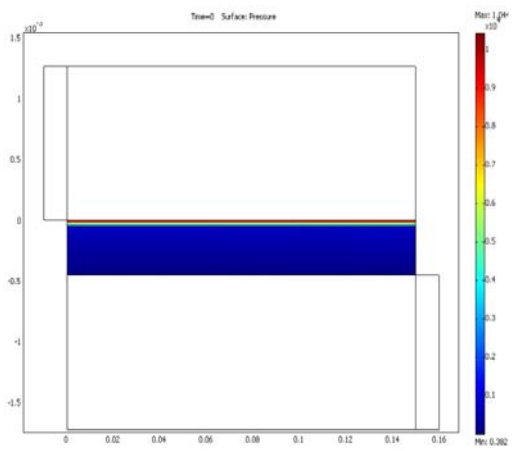

Fig. 5 Soot layer and filter wall pressure distribution at t=0s

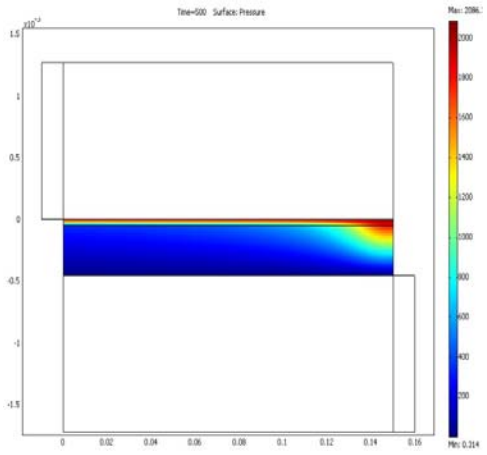

Fig. 6 Soot layer and filter wall pressure distribution at t=500s

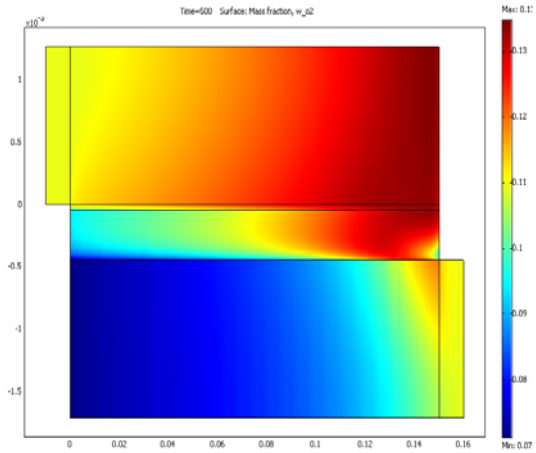

Fig. 7 Oxygen distribution in the filter at t=500s

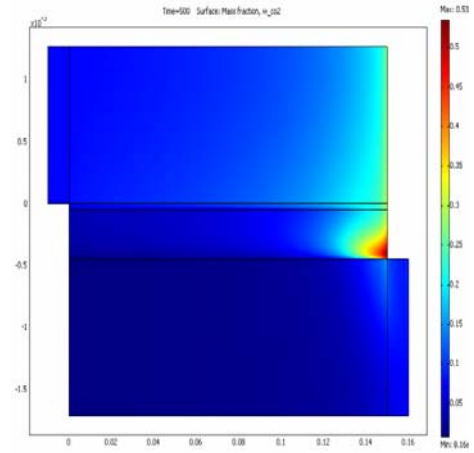

Fig. 8 Carbon Dioxide distribution in the filter at t=500s

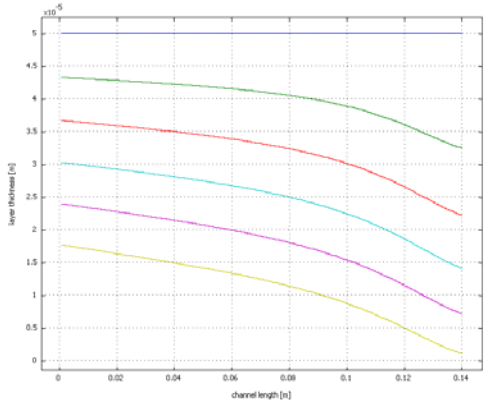

Fig. 9 Soot layer thickness distribution at different times

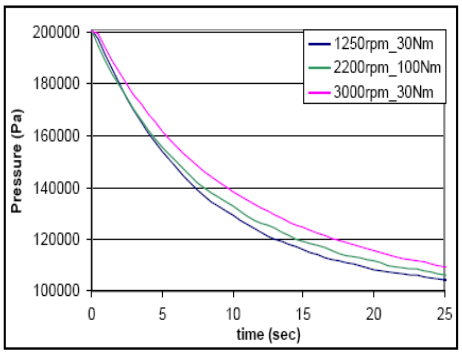

Fig. 10 Exhaust pressure change with time

IV. Validation

To validate the current model, experimental data from Psarianos's work [22] was used. As the major parameter to indicate the effectiveness of the diesel particulate filter regeneration, exhaust backpressure was chosen to be the variable for the validation work. In Psarianos's work, a pressure-time diagram was presented to indicate the DPF regeneration process from the point of view of the exhaust backpressure in the filter. When the filter is loaded with soot, the exhaust backpressure will continue to increase until the soot layer starts to burn.

As the soot layer in the filter gradually burns off, the exhaust pressure in the filter will be supposed to decrease. Figure 10 from Psarianos's work clearly shows this trend at different engine operating points. Figure 11 shows the calculated exhaust backpressure change with time from FEMLAB at one point in the inlet channel of the particulate filter. Obviously, the calculated results exhibits similar pressure change trend as the experimental data. Therefore, according to the above comparison, the current model shows valid results.

To further the validation, chemical reactions have been turned off from the current model. Under this situation, there should be almost uniform soot layer thickness distribution along the channel at all the time. The soot layer thickness should also expect to increase as the time goes on since there is no soot layer oxidation reaction. Figure 12 shows the soot layer thickness distribution along the channel at different time. As can be seen, the results are almost the same as expected. Thus, at this point, the current model is believed to be valid.

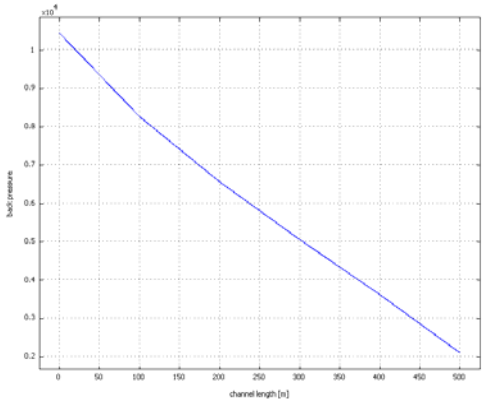

Fig. 11 Calculated exhaust pressure in the filter

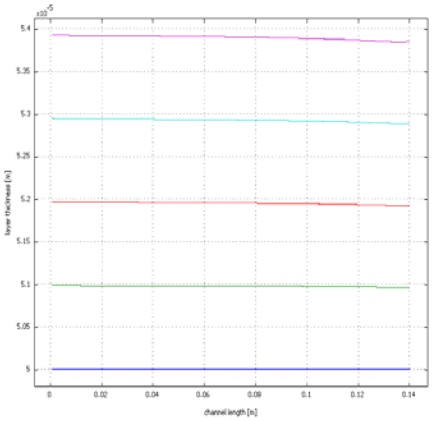

Fig. 12 Soot layer thickness distribution at different time

V. Parametric Study

Since engine exhaust temperature is a crucial parameter for the soot layer oxidation reactions and it greatly affects the engine fuel consumption, it is selected as the variable for parametric study. It is of great interest to know at what temperature the soot layer oxidation process starts to accelerate significantly and how sensitive the soot layer thickness is related to the engine exhaust temperature. The goal of doping additive in the diesel fuel is to reduce the effective engine exhaust temperature and thus reduce the engine fuel consumption. For this parametric study, the situation of fuel doped with cerium catalyst condition is considered. Figure 13 shows how soot layer thickness distribution along the filter channel relates to the engine exhaust temperature at the time of 20 seconds.

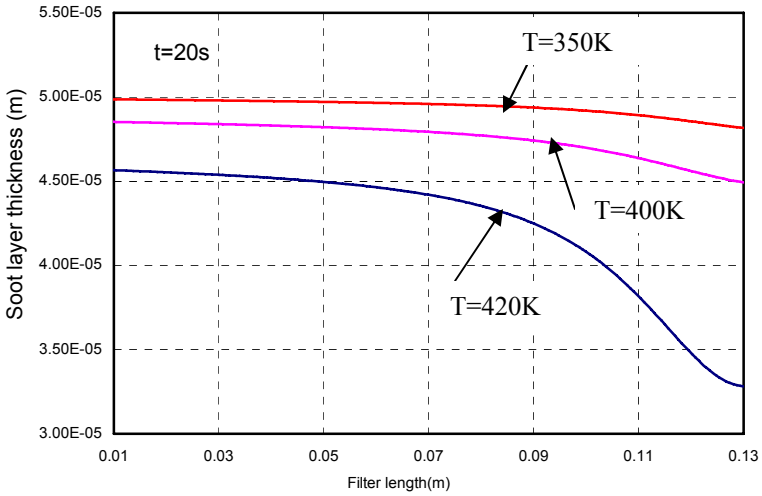

Fig 13. Soot layer thickness distribution at t=20s

From this figure, it can be seen that when the exhaust temperature is below 400 °C, the exhaust temperature effects on soot layer oxidation is not significant. However, when the temperature goes beyond 400 °C, even a small increase in exhaust temperature will result in a significant increase in the soot layer oxidation reaction rate which in turn reduces the soot layer thickness to a greater extent. Therefore, as can be seen from the above discussion, exhaust temperature has a great impact on soot layer oxidation process. When the exhaust temperature is beyond 400 °C, the soot layer thickness is becoming very sensitive to the change of exhaust temperature. The parametric study in exhaust species concentration effects on the soot layer regeneration will be taken into account in the future study.

VI. Conclusion

Based on the previous existed models, a 2D time-dependent diesel particulate filter regeneration model has been formulated. Mass balance, momentum balances, energy balance and catalytic chemical reactions have been taken into account in the current model. Several conclusions can be drawn from this model.

1. Soot layer thickness distribution is non-uniform during the diesel particulate filter regeneration process due to the fact that the temperature is non-uniformly distributed along the filter channel. It is found that the reaction starts from the downstream at the end of the filter channel and then propagates to the upstream. Both pressure distribution and soot layer thickness distribution have shown this fact. At t=500s, it is observed that the soot layer at the end of the filter channel is nearly burned out. The carbon dioxide distribution in the filter also shows that the concentration of carbon dioxide at the end of the filter channel is higher than the one in the upstream locations. Since the carbon dioxide is the product of the soot oxidation, this also indicates the aforementioned the reaction trend.
2. Engine exhaust temperature has a great impact on the soot layer regeneration process. When catalyst is doped in the fuel the required temperature for the soot layer oxidation is lowered. It is observed that, under the fuel doped with catalysts condition, the soot layer thickness starts to be greatly affected by the engine exhaust temperature when the exhaust temperature is beyond 400 °C. Results showed that even a small change in exhaust temperature can result in a significant change in soot layer thickness when the exhaust temperature is beyond 400 °C.
3. Gas phase reaction has not been considered in this model and will be taken into account in the future study. The exhaust gas species concentration effects on soot layer oxidation are also of great interests to be investigated in the future study.

References:

1. Koltsakis, G., Stamatelos, A., "Catalytic Automotive Exhaust Aftertreatment", *Progress in Energy and Combustion Science*, v 23, n 1, 1997, p 1-39.
2. Law M.C., Clarke, A., Garner, C.P., "A Diesel Particulate Filter Regeneration Model with a Multi-step Chemical Reaction Scheme", *Proc. ImechE. Part D: J. Automobile Engineering.* v 219.
3. Johnson, J. H., Bagley, S. T., Gratz, L. D. and Leddy, D. G., " A review of Diesel Particulate Control Technology and of Competition between Oxygen Diffusion and Reaction Emissions Effects, 1992 Horning Memorial Award Lecture", *SAE* 940233.
4. Harano, A., Murata, K., Takamizawa, K. and Sadakata, M., "Oxidation of Carbonaceous Particles in Silent Discharge Reactor", *J. Chem. Engng Japan*, 1998, **31**(5), 700–705.
5. Enga, B., Buchmann, M., Lichtstein, I., " Catalytic Control of Diesel Particulate", *SAE* 820184.
6. Koberstein, E., Pletka, H., Voelker, H., "Catalytically Activated Diesel Exhaust Filters: Engine Test Methods and results", *SAE* 830081.
7. Salvat, O., Marez, P. and Belot, G., "Passenger Car Serial Application of a Particulate Filter System on a Common Rail Direct Injection Diesel Engine", *SAE* 2000-01-0473.
8. Versaevel, P., Colas, H., Rigaudeau, C., Noirot, R., Koltsakis, G. C. and Stamatelos, A. M., "Some Empirical Observations on Diesel Particulate Filter Modelling and Comparison Between Simulations and Experiments. *SAE* 2000-01-0477.
9. Gieshoff , J., Pfeifer, M., Shaefer-Sindlinger, A., Hackbarth, U., Teysset, O., Colignon, C., Rigaudeau, C.," Regeneration of Catalytic Diesel Particulate Filters", SAE 2001-01-0907.
10. Maricq, M., Guo, G., Xu, N., Laing, P. and Hammerle, B., "Performance of a Catalyzed Diesel Particulate Filter System during Soot Accumulation and Regeneration", *SAE* 2003-01-0047.
11. Bissett, E.J., " Mathematical Model of the Thermal Regeneration of a Wall-flow Monolith Diesel Particulate Filter", *Chem. Eng. Sci.,* 1984, 39(7/8), 1233-1244.
12. Bissett, E.J., Shadmann, F., " Thermal Regeneration of Diesel Particulate Monolith Filters", *AIChE J.,* 1985, 31(5), 753-758.
13. Garner, C. P. and Dent, J. C., "A Thermal Regeneration Model for Monolithic and Fibrous Diesel Particulate Traps", *SAE Trans., J. Passenger Cars*, 1988, 97(4), 9–24.
14. Koltsakis,G. C., Stamatelos, A.M., *American Institute of Chemical Engineers*, 42: 1662(1996).
15. Opris, C. N. and Johnson, J. H., " A 2-D Computational Model Describing the Heat Transfer, Reaction Kinetics and Regeneration Characteristics of a Ceramic Diesel Particulate Trap", *SAE* 980546.
16. Konstandopolous, A. G., Kostoglou, M., Housiada, P., Vlachos, N., and Zarvalis, D., " Multichannel Simulation of Soot Oxidation in Diesel Particulate Filters", SAE 2003-01-0839.
17. Law M.C., Clarke, A., Garner, C.P., " The Effects of Soot Properties on Regeneration Behavior of Wall-flow Diesel Particulate Filters", *Proc. ImechE. Part D: J. Automobile Engineering.* v. 218.
18. Koltsakis,G. C., Stamatelos, A.M, " Computer Aided Engineering of Diesel Filter Systems", *Joint Meeting of the Italian and the Greek Section of the Combustion Institute, 17- 19 June 2004,* Corfu Island, Greece.
19. Koltsakis, G., Stamatelos, A.,: *Ind. Eng. Chem. Res.*, 36:4155 (1997)
20. Pontikakis, G., " Modeling, Reaction Schemes and Parameter Estimation in Catalytic Converters and Diesel Filters", PhD Thesis, University of Thessaly (2003).
21. Stratakis,G., Pontikakis,G., Stamatelos, A., *Proc. Instn. Mech. Engrs. Part D*, 218:203 (2004).

22. Psarianos, "Development of a System for the Measurement of Soot Maldistribution and Pressure Drop Characteristics in Diesel Particulate Filter", *Master's Thesis* , 2002